On the distribution of the heat transfer coefficient in turbulent and "transitional" wedges

J. P. Clark, P. J. Magari and T. V. Jones

Department of Engineering Science, Oxford University, Oxford, UK

The distribution of the heat transfer coefficient in a turbulent wedge was mapped in a low-speed induced-flow tunnel fitted with a heated flat plate instrumented with liquid crystals. Wedges were generated by both a three-dimensional roughness on the flat-plate surface and a wire placed upstream of the leading edge of the plate and oriented orthogonally to it. It was found that the wake-induced wedge was fundamentally different from that initiated by the roughness element. While the wedge induced by the roughness element had all the characteristics of the turbulent wedge as described by other researchers, the wake-induced wedge was more aptly termed a *transitional wedge*. This term was applied to the wedge produced by the impinging wake because the heat transfer distribution was more characteristic of that measured in a transitional zone than that observed in an artificially tripped boundary layer. It was conjectured from the heat transfer contours that the transitional wedge consisted of a series of discrete turbulent spots that grew and coalesced as they convected in the streamwise direction. The suspected intermittent nature of the boundary layer in the transitional wedge was confirmed by hot-wire measurements. The transitional wedge spread laterally at roughly the same angle as the turbulent wedge, and the angle was much larger than the spreading angle of the wake from the wire. This particular transition phenomenon has not been reported previously.

Keywords: boundary layers; transition; turbulent wedge

Introduction

If a three-dimensional (3-D) roughness element of sufficient size is placed in a laminar boundary layer, it can induce an immediate transition to turbulence in the form of a wedge of turbulent fluid with its vertex located at the protuberance location. As it moves downstream, this turbulent wedge spreads laterally at an angle much larger than that of a turbulent wake emanating from the particle and roughly equal to the spreading angle of a turbulent spot. Charters (1943), who was the first to call attention to this form of transition mechanism, termed it "transverse contamination."

The turbulent wedge is a form of bypass transition that has been observed in a variety of different flows. For instance, transition via the turbulent wedge was studied on a flat plate at subsonic speeds by Schubauer and Klebanoff (1955). More recently, Gad-el-Hak et al. (1981) studied the turbulent wedge on a flat plate towed through a water channel. Also, turbulent wedges have been observed downstream of 3-D roughness elements on winglets operating at transonic velocities (Holmes 1986). In addition, they were noted in hypersonic flow as being the transition mechanism at work on the blunt noses of reentry vehicles being designed in the 1950s (Morkovin 1985).

The spreading angle of a turbulent wedge in low-speed flow has been determined by a number of researchers with excellent consistency. The shape of a turbulent wedge as measured by Schubauer and Klebanoff (1955) using hot-wire anemometry is illustrated in Figure 1. They found that the turbulent wedge consists of a fully turbulent core that spreads at a half angle of 6.4° from the free-stream direction. They also found that this fully turbulent core is bounded by an intermittent region that subtends an angle of 10.6° with the free-stream direction. They concluded that a 3-D roughness simply causes a continual production of turbulent spots, which then travel downstream as would turbulent spots produced by any other mechanism.

An important parameter in determining whether a 3-D roughness element of a given size will trip the boundary layer is the roughness Reynolds number, defined by White (1992) as

$$\mathrm{Re}_r = \frac{u(r)r}{\nu} \tag{1}$$

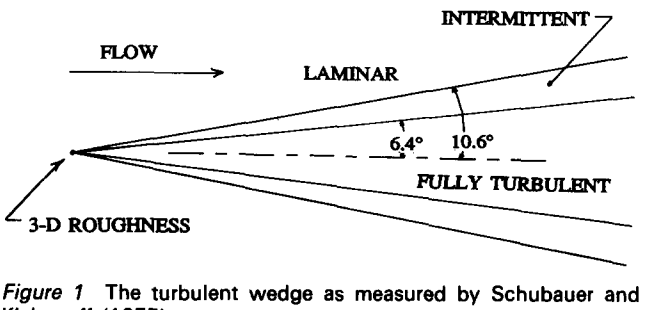

Figure 1 The turbulent wedge as measured by Schubauer and Klebanoff (1955)

Address reprint requests to Professor Jones at the Department of Engineering Science, Oxford University, Parks Road, Oxford OX1 3PJ, UK.

Received 31 May 1991; accepted 17 September 1992

where r is the roughness height, $u(r)$ is the x-component of velocity in the boundary layer at the roughness height, and ν is the kinematic viscosity of the fluid. If $Re_r > 600$, the boundary layer is fully tripped by the roughness, and a turbulent wedge is formed immediately downstream of the excrescence. However, if Re_r is somewhat less than 600, a turbulent wedge can be formed whose vertex is some distance downstream of the roughness element.

Morkovin (1985) points out that there is another criterion that must be satisfied if a boundary layer is to be tripped by a 3-D roughness and a turbulent wedge formed. He states that the 3-D roughness must also be at a location in the boundary layer where turbulent bursting can be sustained. Since there is a minimum momentum-thickness Reynolds number ($Re_{\theta,min}$) below which the bursting process will not persist, there is also an $Re_{\theta,min}$ below which transition caused by a 3-D roughness will not sustain itself, and the boundary layer will thus relaminarize. However, above this $Re_{\theta,min}$, which for a flat plate corresponds roughly to the critical momentum-thickess Reynolds number for small disturbances, a 3-D roughness will initiate a turbulent wedge, and transition will take place by transverse contamination.

Some interesting observations concerning the turbulent wedge were reported by Gad-el-Hak et al. (1981). Using dye flow-visualization and a flat plate towed through a water channel, they were able to determine the mechanism by which a turbulent wedge spreads laterally. They coated a 3-D roughness element with dye of one color and then proceeded to seep dye of another color into the boundary layer across much of the span of the plate. As a result, they were able to visualize the spread of the wake from the roughness as well as the lateral propagation of the wedge front simultaneously. They observed the wake of the roughness spreading at an angle very much smaller than that of the turbulent wedge. From this, they concluded that the mechanism by which transverse contamination takes place is the localized destabilization of the boundary layer adjacent to turbulent spots convecting downstream from the roughness. This implied that the lateral propagation of turbulent spots in general was also governed by a local destabilization of the boundary layer in their vicinity. They termed this mechanism "growth by destabilization."

In this study, a phenomenon quite similar to the turbulent wedge is described. Although the observed phenomenon, termed a *transitional wedge*, is similar in many regards to the turbulent wedge, there are certain fundamental differences between the two that are detailed. The distribution of the heat transfer coefficient in a turbulent wedge was mapped using the heated-coating method for the measurement of local heat transfer coefficients and compared to that obtained in a transitional wedge. The wedges were initiated in an otherwise laminar boundary layer on a flat plate at a low subsonic speed via two means. The turbulent wedge was generated by placing a 3-D roughness element on the plate surface, and the transitional wedge was formed by placing a wire orthogonal to and upstream of the leading edge of the plate. At first glance, the wedges formed appeared to be the same. However, closer inspection of the measured distributions of the heat transfer coefficient in the wedges revealed certain fundamental differences between them.

Experimental technique

The experiment was performed in a low-speed induced-flow wind tunnel, described in detail by Mohandes (1979). The working section of the tunnel was fitted with a vertically oriented perspex flat plate with an elliptical leading edge (see Figure 2). The free-stream velocity in the test section of the tunnel was measured to be 43.1 m/s, and the free-stream turbulence intensity in the tunnel was on the order of 0.3 percent. The free-stream velocity in the test section varied by as much as 2 percent over the surface of the plate, but remained essentially constant over the instrumented portion of the test surface.

Turbulent wedges were generated on the plate by two means. First, a 3-D roughness (1 mm-diameter ball bearing) was placed 60 mm downstream of the leading edge of the plate. The roughness Reynolds number, Re_r, was estimated to be 2850 at

Notation

A	Area (m^2)
c_p	Specific heat (kJ/kg K)
D	Diameter of wire (m)
h	Convective heat transfer coefficient (W/m^2 K)
k	Thermal conductivity (W/m K)
I	Current (A)
Nu_x	Local Nusselt number, hx/k
Pr	Prandtl number, $\mu c_p/k$
q	Heat flux (W/m^2)
R	Resistance (Ω/m^2)
r	Roughness height (m)
Re_D	Wire Reynolds number, $U_\infty D/\nu$
Re_r	Roughness Reynolds number, $u(r)\, r/\nu$
Re_x	Length Reynolds number, $U_\infty x/\nu$
Re_θ	Momentum thickness Reynolds number, $U_\infty \theta/\nu$
T	Temperature (K)
t	Thickness of perspex plate (m)
Tu	Turbulence intensity, u'/U_∞ (percent)
U	Streamwise component of velocity (m/sec)
x	Streamwise distance from plate leading edge (m)
y	Normal distance from flat-plate surface (m)
z	Spanwise distance along plate (m)
ε	Emissivity
θ	Momentum thickness (m)
Λ_x	Integral length scale in streamwise direction (m)
μ	Dynamic viscosity (Pa s)
ν	Kinematic viscosity (m^2/sec)
σ	Stefan–Boltzman constant (5.67×10^{-8} W/m^2 K^4)

Subscripts

cv	Convection
cd	Conduction
cr	Critical
lc	Liquid crystal
o	Total quantity
r	Roughness
rd	Radiation
tr	Transition
w	Wall quantity
x	Measured from leading edge
∞	Freestream quantity

Superscripts

′	Fluctuating component

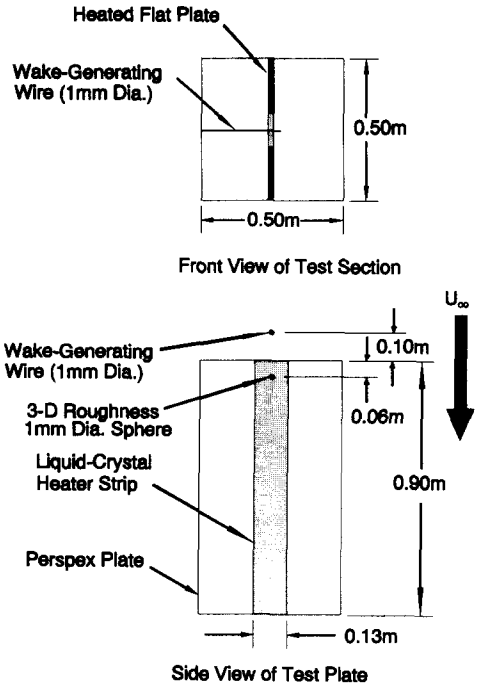

Figure 2 Schematic of the test section of the low-speed tunnel illustrating the instrumented flat plate. The upstream wire and the 3-D roughness element indicated in the figure were used separately to inject disturbances into the boundary layer

this location. The second turbulent wedge was produced by the impinging wake of a 1-mm diameter wire ($Re_D = 2850$) placed 100 mm upstream of the leading edge of the plate and oriented orthogonally to the plane of the plate (also shown in Figure 2). At the leading edge of the plate, the turbulence intensity in the wake was measured to be 3 percent, and the streamwise integral length scale, Λ_x, was estimated to be on the order of the wire diameter.

The center of one side of the perspex plate was fitted with a metallized polymer strip that was supplied with current from a variable transformer. It was therefore possible to generate a nearly uniform heat-flux condition over this strip. Varying the current input to the heater strip made it possible to adjust the temperature distribution so that isotherms on the plate could be mapped. Individual isotherms were made visible by applying chiral nematic (thermochromic) liquid crystals to the surface of the heater strip. The particular crystals utilized in this study had a yellow color at a calibrated temperature of 30°C, and the entire color play for the crystals took place over a narrow temperature band of approximately 2°C. Therefore, stepwise changes in the heater input revealed the isotherm at the crystal calibration temperature for a given heater input. Mapping of the heat transfer coefficient over the surface of the plate required only that the isotherms, as indicated by the liquid crystals, be recorded photographically using a VHS recorder. The individually recorded images detailing the isotherms at each of the heater settings were converted to hard copy with the aid of an image processing system (implemented by Z. Wang at Oxford University) and then superimposed into a single plot from which the heat transfer coefficient was determined as outlined below.

The heat transfer coefficient associated with each isotherm can be calculated by performing an energy balance on the surface of the model. The heat flux convected from the surface, q_{cv}, at a given heater current is equal to

$$q_{cv} = q_{in} - q_{rd} - q_{cd} \tag{2}$$

where q_{in}, q_{rd}, and q_{cd} are the input heat flux and the heat fluxes lost via radiation to the surroundings and conduction through the back of the plate, respectively. The input heat flux is, of course,

$$q_{in} = I^2R \tag{3}$$

where I is the input current and R is the resistance per square meter of the heater strip at the calibrated liquid crystal temperature. The heat flux lost via radiation to the surroundings is found from the standard formula for radiant heat transfer in an enclosure

$$q_{rd} = \varepsilon\sigma(T_{lc}^4 - T_o^4) \tag{4}$$

where ε, σ, T_{lc}, and T_o are the emissivity of the model, the Stefan–Boltzman constant, the liquid crystal temperature, and the recovery temperature of the fluid ($\approx$20°C), respectively. Since only one side of the flat plate was heated, the loss due to conduction through the perspex model is

$$q_{cd} = -k(T_o - T_{lc})/t \tag{5}$$

where k is the thermal conductivity of perspex and t is the thickness of the perspex plate. The heat flux convected from the surface is also defined as

$$q_{cv} = h(T_{lc} - T_o) \tag{6}$$

where h is the local heat transfer coefficient. Substituting Equations 3, 4, 5, and 6 into Equation 2 and solving for the heat transfer coefficient gives

$$h = \frac{I^2R - \varepsilon\sigma(T_{lc}^4 - T_o^4) + k(T_o - T_{lc})/t}{T_{lc} - T_o} \tag{7}$$

Equation 7 clearly shows that a line of constant temperature as determined by the liquid crystal corresponds to a line of constant heat transfer coefficient.

The heated-coating method used in this study is very well established and has been fully described by Baughn et al. (1989, 1986, 1985) as well as Hippensteele et al. (1988, 1983). The accuracy of the technique was addressed by Baughn et al. (1989), who showed that the heat transfer coefficient can be determined to within an accuracy of approximately 5 percent using a similar experimental arrangement to the one described here. In this experiment, the maximum surface temperature on the plate was on the order of 50°C. This maximum temperature occurred in the transition region at the highest input heat flux. The maximum temperature variation over the surface of the plate was estimated to be on the order of 20°C.

Results

Figures 3 and 4 are maps of the heat transfer coefficient along the plate for the wedges generated by the 3-D roughness and the wire wake, respectively. The numbers associated with each isotherm increase with increasing heat transfer coefficient. As clearly seen in the figures, the transition zone is somewhat 3-D, and this is to be expected of almost any transition experiment. Ostensibly, both the 3-D roughness-generated wedge and that induced by the wake of the upstream wire are quite similar. Both wedges have spreading angles consistent with the measurements of Schubauer and Klebanoff (1955) (see Figure 1). However, there are substantial differences between the wedges, and these become apparent upon examination of the heat transfer coefficients associated with the isotherms.

Figure 5 is a plot of Nusselt number versus Reynolds number along the flat plate through the centerlines of the two wedges. For comparison, the variation of Nu_x with Re_x along the

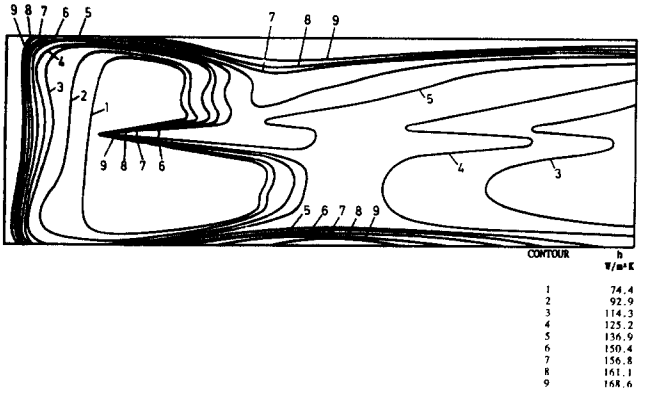

Figure 3 Contours of constant heat transfer coefficient (W/m^2K) for the wedge generated by the 3-D roughness element ($Re_r = 2850$)

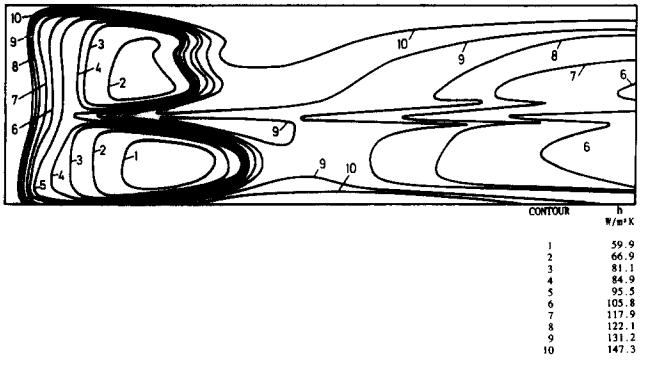

Figure 4 Contours of constant heat transfer coefficient (W/m^2K) for the wedge induced by the impinging wire wake ($Re_D = 2850$)

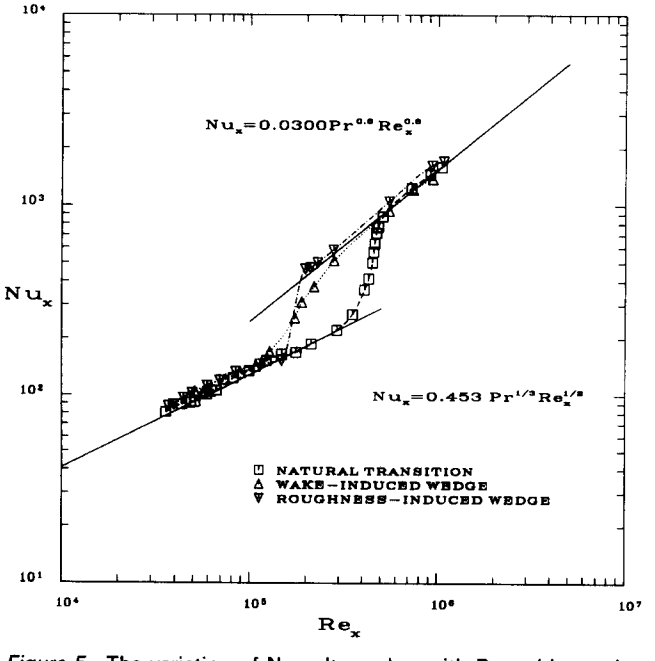

Figure 5 The variation of Nusselt number with Reynolds number along the flat-plate surface for the three transition cases studied

centerline of the flat plate with the boundary layer undergoing "natural" transition to turbulence is also illustrated. For all three of the cases, there is very good agreement between the measured values and the theoretical distributions of Nusselt number along a flat plate with constant heat flux in laminar and fully turbulent boundary layers. The theoretical relations are taken from Kays and Crawford (1980) and are defined in the equations below for the laminar and fully turbulent boundary layers:

$$Nu_x = 0.453\ Pr^{1/3}\ Re_x^{1/2} \quad \text{(laminar)} \tag{8}$$

$$Nu_x = 0.03\ Pr^{0.6}\ Re_x^{0.8} \quad \text{(turbulent)} \tag{9}$$

The variation of Nusselt number through the transition zone is different in each case, however. For "natural" transition, it varies smoothly through the transition zone, as expected. In the case of the wedge generated by the 3-D roughness, Nu_x jumps discontinuously from the laminar to the turbulent value upon passing through the vertex of the wedge. This is consistent with the boundary layer being fully tripped. By contrast, the Nusselt number in the wake-induced wedge increases slowly to the turbulent level, but begins to do so at a much lower Re_x than the natural transition case.

The character of the wedge generated by the 3-D roughness is further illuminated by Figure 6. Figure 6 is a plot of the variation of the heat transfer coefficient with streamwise distance along the plate at two different lateral locations in the wedge. In the figure, the data points indicated by an "o" were taken along the centerline of the wedge, while those marked with an "x" were taken off the centerline. Along the centerline of the wedge, the heat transfer coefficient increases discontinuously at the vertex of the wedge, and then begins to fall. This is consistent with the boundary layer being fully tripped by the roughness. Off the centerline, however, h increases with x, which can only happen in a region of intermittent turbulence on a flat plate in constant pressure flow. This implies that the wedge has all the characteristics of Charters' (1943) turbulent wedge as determined by Schubauer and Klebanoff (1955)—that is, it has a fully turbulent core which is bounded by an intermittent zone. These observations were confirmed with a hot wire placed in the boundary layer. It should also be noted that the angles these zones make with respect to the centerline of the wedge are in good agreement with the results of Schubauer and Klebanoff (1955). The isotherms plotted in Figure 3 indicate that the fully turbulent core of the wedge

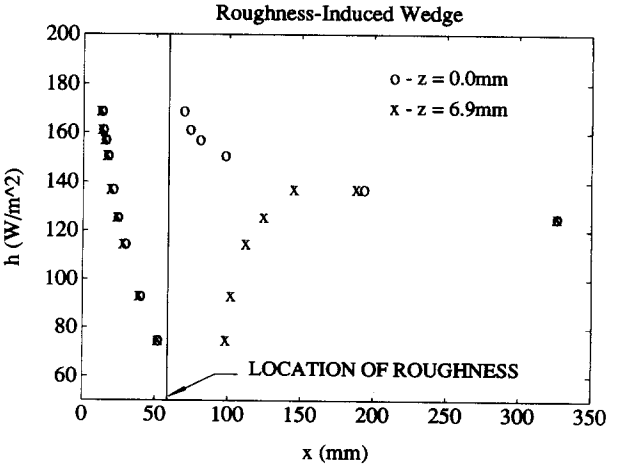

Figure 6 The variation of heat transfer coefficient with streamwise distance along the plate for the roughness-induced wedge

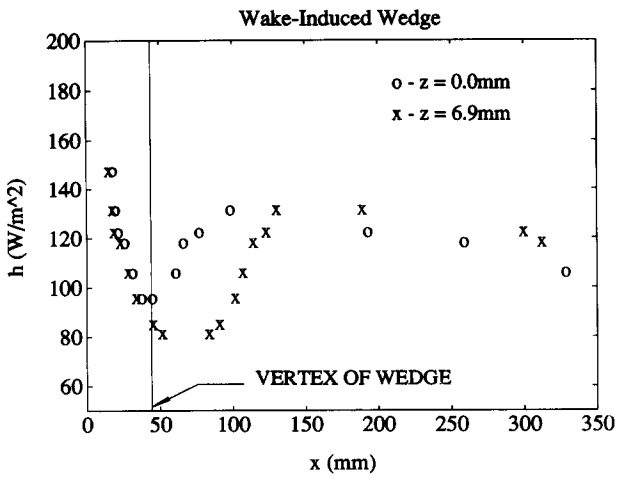

Figure 7 The variation of heat transfer coefficient with streamwise distance along the plate for the wake-induced wedge

spreads at an angle of $\approx 5°$ with the free stream, while the intermittent zone subtends an angle of $\approx 11°$ to the flow.

Several interesting features of the wake-induced wedge are revealed in Figure 7, which is a plot of the variation of h with streamwise distance on and off the centerline of the wedge. For both the centerline and off the centerline, h increases with x. Thus, in contrast with the roughness-induced wedge, there is no fully turbulent core associated with the wedge induced by the wake. Instead, the wake-induced wedge is transitional throughout its entirety. Consequently, this phenomenon is better described as a "transitional wedge" than as a turbulent one. It too has roughly the same overall spreading angle of Charters' (1943) wedge ($\approx 11°$). Again, the transitional nature of the wedge was confirmed with hot-wire measurements.

The experiment was conducted at another free-stream velocity (31.8 m/s) as well. The transitional-wedge phenomenon was repeatable, and all the results were qualitatively similar to those reported here for a free-stream velocity of 43.1 m/s.

Discussion

In each of the three cases tested, transition was initiated in a different manner. In "natural" transition, it was brought about by the natural disturbances present in the flow field. These included, but were not limited to, free-stream turbulence, the surface roughness of the plate, and the heating of the boundary layer by the heater sheet. In the other two instances, one disturbance of the above set played a dominant role. In the case of the 3-D roughness element, the boundary layer was tripped by the excrescence itself. In the wake-induced transition case, the dominant factor was the enhanced turbulence intensity in the wake region downstream of the wire feeding into the boundary layer.

In the course of this experiment, the wedge generated by the upstream wire was studied first. In placing the wire upstream of the leading edge of the plate, it was assumed that a turbulent wedge would form in much the same manner as when a roughness is placed somewhat upstream of $Re_{\theta,min}$, as described by Morkovin (1985). In such an instance, the boundary layer sustains turbulence in the narrow wake of the roughness until such time as $Re_{\theta,min}$ is realized. At that point, the turbulence begins to spread along a front of transverse contamination. Thus, a turbulent wedge is seen to form some distance downstream of the roughness element that causes it.

Even though turbulence must have been sustained in a narrow wake along the flat plate in the case of the wake-induced wedge, the end result was not a turbulent wedge as has been described in the literature previously. Instead, it was a wedge of intermittent turbulence where the transition process was augmented by the receptivity of the boundary layer to the heightened turbulence intensity in the wake of the wire. It was noted that this transitional wedge had approximately the same spreading angle as a roughness-generated turbulent wedge. Furthermore, the transitional wedge spread laterally at an angle much larger than that of the wire wake. Indeed, the measured width of the wedge was 25 mm at a point some 60 mm after its initiation in the boundary layer, while the theoretical width of the wake emanating from the wire was only 9 mm or so at the same location. In addition, as seen in Figure 3, the contours of heat transfer coefficient in the wedge had a linear shape, as opposed to the known parabolic shape of a two-dimensional (2-D) wake.

From the above evidence, it has been conjectured that the major difference between the two wedges is the generation rate of turbulent spots at the apex of the wedges. Many experimenters (e.g., Schubauer and Klebanoff 1955) have believed the turbulent wedge to be the result of turbulent spots emanating continually from a 3-D roughness. The present authors believe the disturbances from the impinging wake also act as a point source for turbulent-spot generation. However, the generation rate of turbulent spots is considerably lower in the case of the impinging wake, and there is thus no fully turbulent core associated with the wedge that results.

It is well known that a flat-plate boundary layer in air is destabilized by the addition of heat. This is most likely the reason for the apparently very rapid transition to turbulence in the "natural" transition case. Similar observations are described by Mee et al. (1991), who have, in fact, quantified the effect of heating on natural transition results in a heated-coating liquid-crystal experiment. However, the addition of heat would have had no effect on the transition point in the case of the roughness-induced wedge. This is because the transition is dominated by the bypass mechanism of the roughness itself, and is therefore all but totally immune to changes in the stability of the laminar boundary layer. Also, it is believed that the same holds true for the wake-induced wedge. In other words, the transitional wedge was not simply the result of the transition zone moving in response to an ever increasing amount of heat in the boundary layer. Were this the case, one would expect the measured isotherms in the wedge to move upstream as more and more heat was added. However, as clearly seen in Figure 4, the isotherms moved downstream when the input heat flux was increased (i.e., at higher values of h). Moreover, Kim et al. (1989), reporting on a very similar experiment to the one described here, stated that the measured start of the transition zone was unaffected by the addition of similar amounts of heat to the boundary layer when the free-stream turbulence intensity was 1.79 percent. Since the transition in this case is brought about by the heightened turbulence intensity in the wake of the wire ($Tu \approx 3$ percent at the leading edge of the plate), it follows that the start of the transition zone (vertex of the wedge) would also be unaffected by the addition of heat.

Figures 8 and 9 provide definitive proof that the transitional wedge is unaffected by changes in the input heat flux. Figure 8 is a plot of unsteady hot-wire traces recorded with the sensor roughly 0.2 mm from the surface of the plate and 75 mm downstream of the leading edge, with the boundary layer undergoing natural transition at two different heater settings. In the top trace, no heat is being added to the boundary layer, and very few turbulent spots are detected by the hot-wire. In

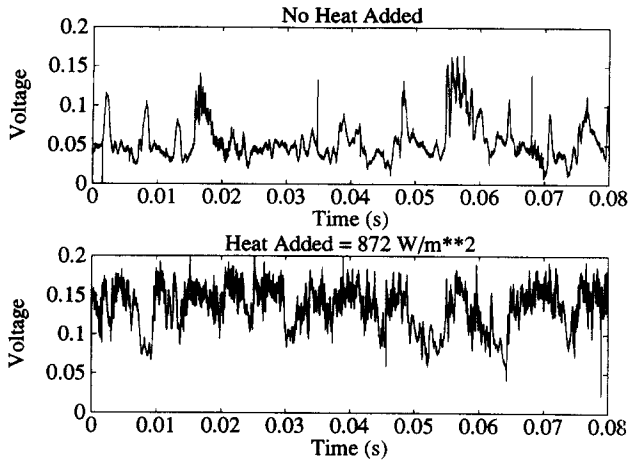

Figure 8 Unsteady hot-wire traces in the boundary layer undergoing "natural" transition with and without heat added

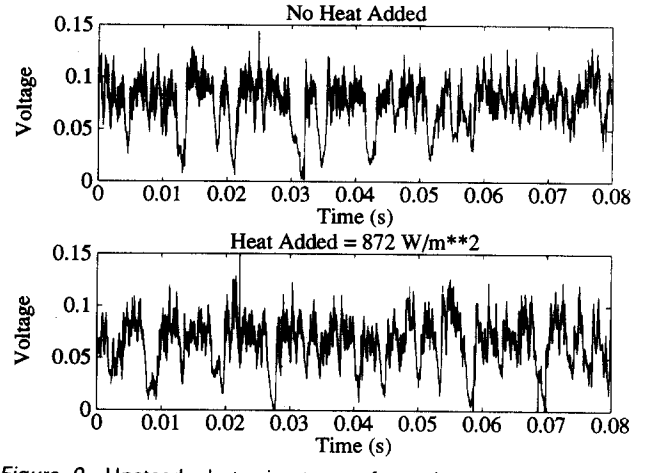

Figure 9 Unsteady hot-wire traces from the centerline of the wake-induced wedge with and without heat added

the lower trace, however, with an input heat flux of 872 W/m^2, there is a marked increase in the intermittency of the signal. Figure 9 is a plot of hot-wire traces recorded at exactly the same conditions and location relative to the plate on the centerline of the wake-induced wedge. It can be seen that the signals are qualitatively the same for both heater settings. This proves that the transitional wedge is not a stability-governed transition. Instead, it is a form of bypass transition that is not substantially affected by the stability of the laminar boundary layer. This confirms that the transitional wedge is a stationary phenomenon illuminated by the heated-coating method of heat transfer measurement and is not caused by the experimental technique itself.

Conclusions

In this study it was found that the character of a wedge of turbulence was quite different depending on how it was induced in the first place. When it was formed via a 3-D roughness element, the distribution of the heat transfer coefficient in the wedge indicated that it had all the characteristics of a classical turbulent wedge. That is, it had a fully turbulent core that was surrounded by a zone of intermittent turbulence making an angle of roughly 11° with the free-stream direction. By contrast, when it was initiated by the wake of a wire placed upstream of the leading edge of the flat plate, it contained no fully turbulent core. Instead, it was a wedge of intermittent turbulence that spread laterally at roughly the same angle as the wedge generated by the roughness. This angle was much larger than the theoretical spreading angle of a turbulent wake. This transition phenomenon has not been reported previously and has been termed the *transitional wedge.*

Acknowledgments

J. P. Clark was supported by the U.S. Air Force Office of Scientific Research under grant 89-0427. P. J. Magari was supported by the National Science Foundation and NATO as an NSF/NATO postdoctoral fellow. Thanks are due to S. R. Smelser and J. S. Takacs for help in the preparation of some of the figures. Also, thanks are due to R. W. Moss, who helped to measure the turbulence quantities reported here, and to Z. Wang, who allowed the authors to make use of his image-processing equipment.

References

Baughn, J. W., Ireland, P. T., Jones, T. V., and Saniei, N. 1989. A comparison of the transient and heated-coating methods for the measurement of local heat-transfer coefficients on a pin fin. *ASME J. Heat Transfer*, **111**, 877–881

Baughn, J. W., Hoffman, M. A., and Makel, D. B. 1986. Improvements in a new technique for measuring local heat-transfer coefficients. *Rev. Sci. Instrum.*, **57**, 650–654

Baughn, J. W., Takahashi, R. K., Hoffman, M. A., and McKillop, A. A. 1985. Local heat transfer coefficient measurements using an electrically heated thin gold-coated sheet. *ASME J. Heat Transfer*, **107**, 953–959

Charters, A. C., Jr. 1943. Transition between laminar and turbulent flow by transverse contamination. NACA TN-891

Gad-el-Hak, M., Blackwelder, R. F., and Riley, J. J. 1981. On the growth of turbulent regions in laminar boundary layers. *J. Fluid Mech.*, **110**, 73–95

Hippensteele, S. A. and Russell, L. M. 1988. High-resolution liquid-crystal heat transfer measurements on the end wall of a turbine passage with variations in Reynolds number. NASA TM-100827

Hippensteele, S. A., Russell, L. M., and Sepka, F. S. 1983. Evaluation of a method for heat transfer measurements and thermal visualisation using a composite of a heater element and liquid crystals. *ASME J. Heat Transfer*, **105**, 184–189

Holmes, B. J., Croom, C. C., Gall, P. D., Manuel, G. S., and Carraway, D. L. 1986. Advanced transition measurement methods for flight applications. AIAA Paper No. 86-9786

Kays, W. M. and Crawford, M. E. 1980. *Convective Heat and Mass Transfer.* McGraw-Hill, New York

Kim, J., Simon, T. W., and Kestoras, M. 1989. Fluid mechanics and heat transfer measurements in transitional boundary layers conditionally sampled on intermittency. *Proc. 1989 Natl. Heat Transfer Conf.*, **HTD-107**, 69–81

Mee, D. J., Walton, T. W., Harrison, S. B., and Jones, T. V. 1991. A comparison of liquid crystal techniques for transition detection. AIAA Paper No. 91-0062

Mohandes, M. A. 1979. The flow through heat exchanger banks. D. Phil. thesis, Oxford University

Morkovin, M. V. 1985. Bypass transition to turbulence and research desiderata. *Transition in Turbines*, NASA CP-2386

Schubauer, G. B. and Klebanoff, P. S. 1955. Contributions on the mechanics of boundary layer transition. NACA TN-3489

White, F. M. 1992. *Viscous Fluid Flow.* McGraw-Hill, New York